Ultrafast photonic crystal nanocavity laser

HATICE ALTUG[1]*, DIRK ENGLUND[1] AND JELENA VUČKOVIĆ[2]

[1]Applied Physics Department, Stanford University, Stanford, California 94305, USA
[2]Electrical Engineering Department, Stanford University, Stanford, California 94305, USA
*e-mail: altug@stanford.edu

Published online: 1 July 2006; doi:10.1038/nphys343

Spontaneous emission is not inherent to an emitter, but rather depends on its electromagnetic environment. In a microcavity, the spontaneous emission rate can be greatly enhanced compared with that in free space. This so-called Purcell effect can dramatically increase laser modulation speeds, although to date no time-domain measurements have demonstrated this. Here we show extremely fast photonic crystal nanocavity lasers with response times as short as a few picoseconds resulting from 75-fold spontaneous emission rate enhancement in the cavity. We demonstrate direct modulation speeds far exceeding 100 GHz (limited by the detector response time), already more than an order of magnitude above the fastest semiconductor lasers. Such ultrafast, efficient, and compact lasers show great promise for applications in high-speed communications, information processing, and on-chip optical interconnects.

The spontaneous emission (SE) rate in a microcavity is enhanced by the Purcell factor[1] (F), proportional to the ratio of the cavity quality factor (Q) to mode volume (V_{mode}). Until now, the advantages of large SE rate enhancement have not been fully explored in lasers because of their large mode volumes. Thus, their SE properties have been dictated by the intrinsic radiative lifetime of the bulk material. With the recent advances in semiconductor fabrication and crystal growth, it has become possible to produce high-quality photonic crystals. These are structures of alternating refractive index[2,3] that provide unprecedented control over the electromagnetic environment. Cavities introduced into the photonic crystal can have extremely high Q/V_{mode} ratios, and therefore can enable large Purcell factors. So far, such nanocavities have been used for cavity quantum electrodynamic (QED) experiments[4–12] such as SE rate enhancement[4,5,9–11] and suppression[4], and also for single-photon sources[4,12] and lower-threshold lasers[13–17]. Here, we demonstrate extremely fast photonic crystal nanocavity lasers with response times below the 2 ps detection limit of our measurement apparatus. The turn-on delay times are measured as near 1 ps, more than an order of magnitude faster than previous measurements[18,19].

There are two important laser modulation schemes: small- and large-signal modulation. We analyse the laser dynamics by solving the laser rate equations[20] for photon and carrier densities. Communication systems use both small- and large-signal modulation[20–22]. In the small-signal regime, the laser is driven with an above-threshold d.c. pump power $L_{\mathrm{in},0}$ and modulated with a small time-varying (a.c.) signal ΔL_{in}. The carrier and photon densities follow the pump with d.c. and a.c. components $N_0 + \Delta N$ and $P_0 + \Delta P$, respectively. The modulation response is given by $\Delta P/\Delta N$. At low d.c. driving power above threshold, the bandwidth of the laser is limited by the relaxation oscillation frequency:

$$\omega_{\mathrm{R}}^2 = \frac{a v_{\mathrm{g}} P_0}{\tau_{\mathrm{p}}} + \frac{\beta}{(\tau_{\mathrm{p}}\tau_{\mathrm{r0}}/F)} + \frac{\beta N_0}{(\tau_{\mathrm{r0}}/F)P_0}\left(\frac{1}{\tau_{\mathrm{total}}} - \frac{1}{\tau_{\mathrm{r0}}/F}\right). \quad (1)$$

Here, the parameters are as follows: τ_{r0} is the intrinsic carrier radiative lifetime of the bulk material, a is the differential gain, v_{g} is the group velocity, τ_{p} ($=Q/\omega_{\mathrm{l}}$) is the photon lifetime, ω_{l} is the lasing frequency, β is the SE-coupling factor, τ_{nr} is the non-radiative lifetime, and $1/\tau_{\mathrm{total}} = F/\tau_{\mathrm{r0}} + 1/\tau_{\mathrm{nr}}$.

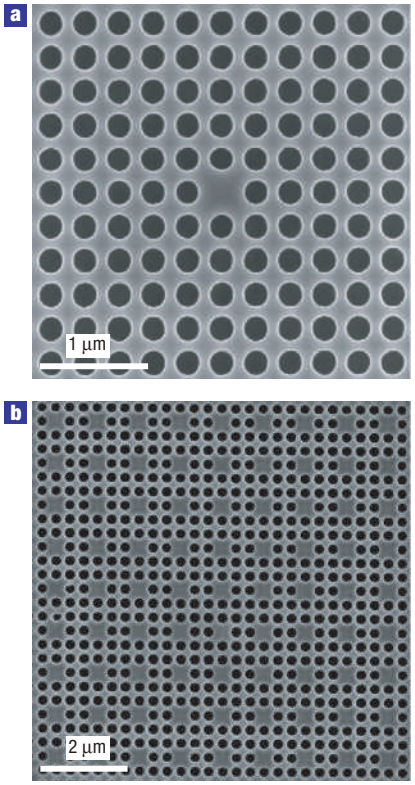

Figure 1 Scanning electron micrographs of fabricated structures. **a**, Single-defect photonic crystal cavity laser with six PhC confining layers around the defect. **b**, Coupled-cavity array laser consisting of a 9×9 array in the described GaAs material system. The periodicity of the holes is fixed at 315 nm, and the hole radius is tuned from 105 to 130 nm to change the resonance frequency of the cavities.

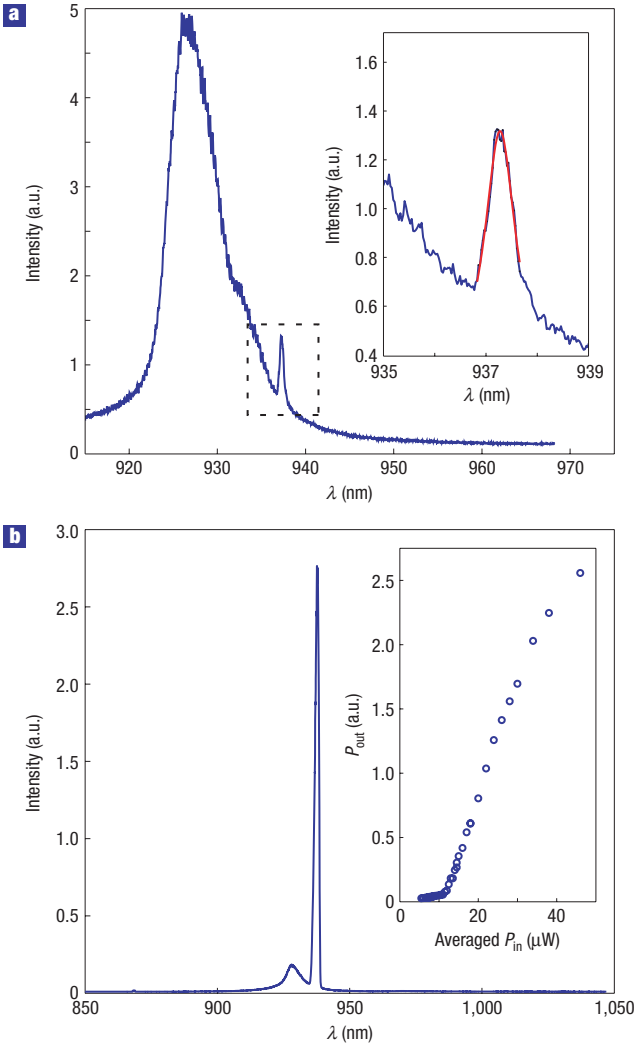

Figure 2 Spectra of the single-defect photonic crystal laser. **a**, Spectrum below lasing threshold. The dashed rectangle indicates the cavity mode, and the inset shows the lorentzian fit (red) for its Q-factor estimation. **b**, Spectrum above threshold. The inset shows the lasing curve, that is, the input pump power versus output power.

In conventional semiconductor lasers, the fraction of spontaneously emitted photons that is coupled into a single-cavity mode (denoted by β) is small due to the small F factor[20]. Therefore, only the first term in equation (1) is considered[20]. The standard way to improve modulation bandwidth is to increase the photon density (P_0) with stronger pumping. However, this causes significant thermal problems and practically limits the modulation speeds to below 20 GHz (ref. 22). On the other hand, in nanocavity lasers with large Purcell effect, β can approach unity while the intrinsic radiative lifetime is reduced dramatically (that is, F is large). This makes the additional terms in (1) significant. Thus, these cavity-QED effects open a fundamentally new pathway for improving laser modulation bandwidth[23].

In the strong-pumping regime, the bandwidth is determined by the cavity ring-down time τ_p. Although the cavity effects could be increased with higher Q, the longer photon lifetime would still limit modulation speeds significantly. For example, for $Q = 10^6$ ($\tau_p \sim 50$ ps), the modulation speed is only 20 GHz. Thus, ultrahigh Q cavities[24] (such as microdiscs) alone cannot achieve higher modulation speeds. In contrast, photonic crystal nanocavities enable very large Purcell effects, even with moderate Q values, because of their ultrasmall cavity mode volumes, below (λ/n) (ref. 3). In our lasers with large Purcell factor, the Q values can be as small as several thousand, allowing fast cavity ring-down times ($\tau_p < 1$ ps).

In large-signal modulation, where the laser is turned on and off completely, our QED-enhanced lasers offer particularly striking advantages. For this modulation scheme, an important parameter is the turn-on delay time[18–20], which is the time delay between the pump and laser peak responses. Turn-on delay times severely limit laser speeds. The delay time can be significantly decreased if the stimulated emission process is faster, which can be achieved in a cavity with large β value and large SE rate enhancement. Increasing pump power can also reduce the delay time[18] at the expense of thermal problems, reduced laser reliability and significant chirp. This delay time is limited to a few tens of picoseconds in fast semiconductor lasers[18,19], but it is reduced more than an order of magnitude in our QED-enhanced nanocavity lasers even at power levels near lasing threshold. We have measured delay times as small as 1.5 ps for pump powers only 1.3 times above lasing threshold.

Besides the dramatically enhanced small- and large-signal modulation speeds, the QED-enhanced lasers can also significantly improve power consumption[13–17,23] and associated thermal

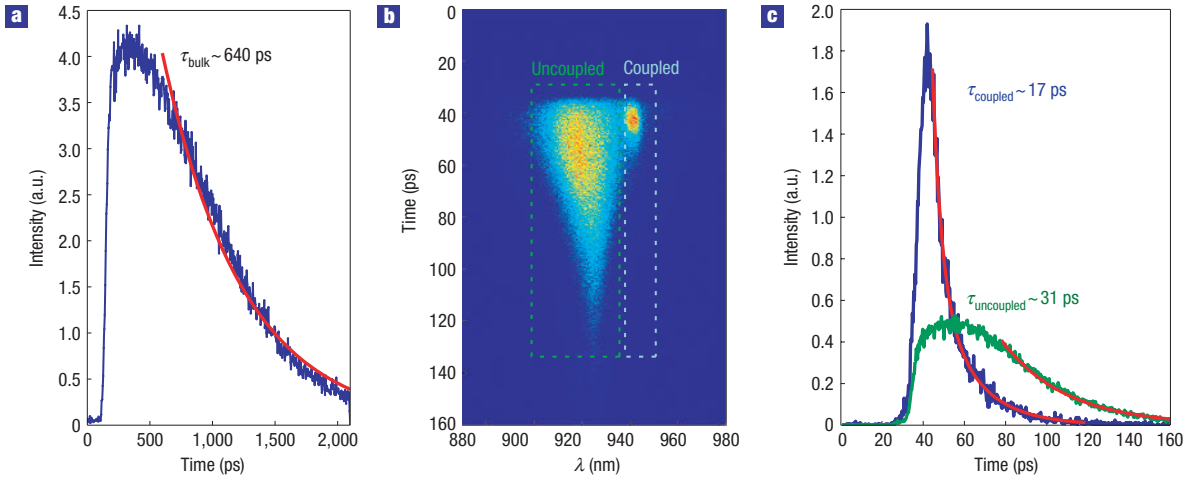

Figure 3 Time-resolved photoluminescence decay curves measured by streak camera. a, For the $In_{02}Ga_{0.8}As$ MQW structure in bulk (unpatterned MQW region) with an exponential fit (red). **b**, For the photonic crystal coupled-cavity array laser below lasing threshold. The lobes at the longer (943 nm) and shorter (925 nm) wavelengths correspond to coupled and uncoupled carriers to the cavity mode, respectively. **c**, The decay curves of carriers shown with dashed rectangles in **b** with exponential fits.

problems. The large β reduces the threshold power of the laser[23]. In addition, the use of small mode volume cavities increases the photon density, so the modulation speed can be increased without increasing the pump power.

Our nanocavity laser is based on a 2D photonic crystal slab patterned with a square lattice. Lattice defects in the form of missing holes act as cavities to confine light. Both single- and coupled-nanocavity array structures[25,26] are fabricated on a 172-nm-thick GaAs layer by a combination of electron beam lithography, and dry and wet etching[4] (Fig. 1). The slab contains a gain medium consisting of four 8-nm $In_{0.2}Ga_{0.8}As$ multiple quantum wells (MQW) separated by 8-nm GaAs barriers.

The lasers are optically pumped by 170-fs short pulses with a repetition rate at 80 MHz and wavelength centred at 750 nm using a confocal microscope[4]. The spectrum and time response of the PhC lasers are measured with a spectrometer and a streak camera, respectively. The streak-camera time response is limited to 3–4 ps linewidth, as measured with a 170-fs laser pulse. Because the spectral response of the streak camera drops rapidly below 950 nm, we chose the GaAs-based laser material system. At room temperature, the peak photoluminescence emission wavelength of the quantum wells is at 980 nm. We cooled the sample in a cryostat to 7–150 K to improve overlap between the cavity resonances and the MQW gain. The cooling also improved heat dissipation from the photonic crystal membranes, although we also observed high-speed lasing at room temperature at lower repetition rates.

We observed single-mode lasing from both single- and coupled-cavity array structures. Figure 2 shows the single-cavity spectra below and above threshold. The below-threshold spectrum indicates a Q value of 1,200 from a lorentzian fit (Fig. 2a, inset). The resonant mode has dipole polarization symmetry. Its mode volume is calculated as $0.55\,(\lambda/n)^3$. The same set of measurements on coupled-cavity array structures yielded Q values near 900. From their threshold ratio, we estimate the mode volume of coupled-cavity array laser to be nearly 10 times larger than that of single cavity[26]. Therefore single cavities, by having larger Q/V_{mode} ratios, should achieve much larger Purcell factors.

To estimate the cavity Purcell factor F, we measured the decay rates of the carriers in the bulk (unpatterned MQW region) and in the photonic crystal for cavity-coupled and uncoupled cases. These rates obey the following equations:

$$\frac{1}{\tau_{bulk}} = \frac{1}{\tau_{r0}} + \frac{1}{\tau_{bulk,nr}};$$
$$\frac{1}{\tau_{coupled}} = \frac{F}{\tau_{r0}} + \frac{1}{\tau_{PhC,nr}};$$
$$\frac{1}{\tau_{uncoupled}} = \frac{1}{\tau_{r0}} + \frac{1}{\tau_{PhC,nr}}. \qquad (2)$$

We estimate the decay times for the cavity array structure from Fig. 3. The radiative bulk carrier lifetime (τ_{r0}) is at least 640 ps (Fig. 3a). For bulk, we can neglect non-radiative processes ($\tau_{bulk,nr}$) as they are much slower than the radiative processes. The radiative decay rates for cavity-coupled and uncoupled carrier emission in the PhC-patterned region are $\tau_{coupled} \sim 17$ ps and $\tau_{uncoupled} \sim 31$ ps (Fig. 3b,c). Uncoupled emission is faster than bulk carrier lifetime because of the increased non-radiative recombination rate ($1/\tau_{PhC,nr}$) owing to the enhanced surface recombination in the patterned structures. The cavity-coupled emission is even faster as the Purcell-enhanced radiative emission rate (F/τ_{r0}) outpaces non-radiative recombination. By solving (2) with these measured values, we estimated the in-plane-averaged SE rate enhancement (F) for the cavity array structure to be 17. The inclusion of SE rate suppression[4] of uncoupled carriers in photonic crystal (which is neglected here) will further increase F. Such high Purcell factors in coupled array lasers enable both fast laser response, as well as high output powers with single-mode operation[26]. Repeating these measurements for the single-defect cavity, we obtained $\tau_{coupled} \sim 6.7$ ps, $\tau_{uncoupled} \sim 33$ ps, and in-plane-averaged F as 76. The high Purcell factor for single cavities[4] is not surprising as they are expected to have a maximum F of 165 for the cavity with this set of Q and V_{mode}.

Above lasing threshold, the decay time is reduced another order of magnitude due to stimulated emission. Figure 4a,b shows the time data for the single-defect cavity and coupled-cavity array lasers, respectively. The decays for both lasers are fitted

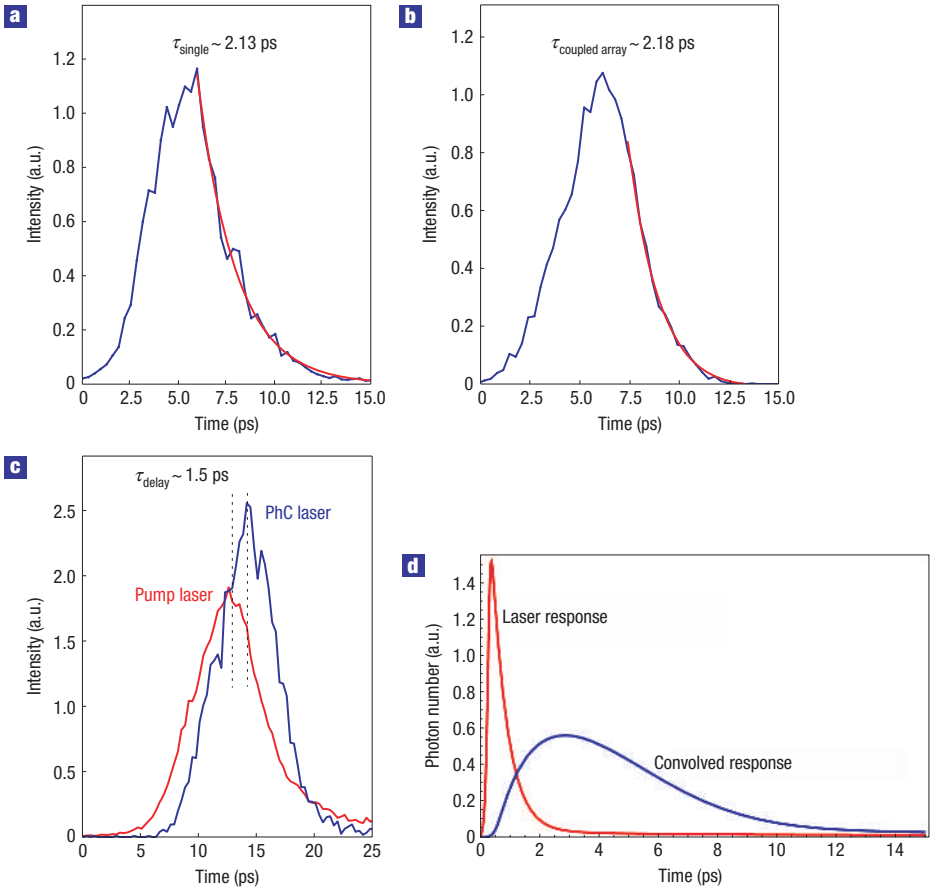

Figure 4 Response of photonic crystal laser. Decay rates above lasing threshold. **a**,**b**, Time response (blue) of a single-defect cavity (**a**) and coupled-cavity array (**b**) laser at 7 K with an exponential fit (red). **c**, Delay-time measurement of a single cavity laser (blue) with respect to pump laser (red). The cryostat temperature was raised from 7 to 100 K to increase the relaxation rate of carriers from upper quantum-well levels to the lowest level by increasing phonon population. At 7 K, the delay time was 3–4 ps, whereas at 100 K, the delay time decreased to 1.5 ps. **d**, Simulated photon number as a function of time for a single-defect cavity laser (red line). The simulation result is convolved with a gaussian of 4-ps width (blue line) to take into account streak-camera response.

by exponentials with a decay constant of 2 ps. To understand the dynamics, we used the laser rate equations to simulate the photon and carrier densities as functions of time. Initially, the photon and carrier densities are taken as zero and above the transparency condition, respectively. The simulated photon density is also convolved with a gaussian of 4-ps width to take into account streak-camera response. The simulation results are shown in Fig. 4d. The bare photon response (unconvolved data) shows that when the laser is pumped above threshold, the photon density decays with the cavity decay time (τ_p). For both the single- and coupled-cavity array lasers, this is 0.5 ps (for Q of 1,000), which is below the resolution limit of our streak camera. The convolved photon response shows a decay time of 2 ps, which agrees well with our experimental results.

As we indicated above, an important parameter in this type of laser modulation scheme is the delay time, which decreases in high Purcell-factor cavities. We measured this delay time at 100 K (with 890-nm pump wavelength) as 1.5 ps (shown in Fig. 4c), close to the streak-camera resolution limit. The delay time is nearly two orders of magnitude shorter than the previous measurements[18,19].

These results already show that single-defect cavity and coupled-cavity array lasers, with τ_p near 0.5 ps and delay time of 1 ps, can be modulated at rates approaching THz. To further demonstrate high-speed characteristics, we directly modulate single-defect cavity lasers at very high speeds by pumping with a series of femtosecond pulses that we generate using a Fabry–Perot etalon. The spacing of the pulse train is controlled by the mirror separation. Only the first three pump pulses have sufficient power to turn on the nanocavity laser. Figure 5 shows the results for the direct modulation of a nanocavity laser above 100 GHz. The response of the laser nicely follows the pump, whose peaks are separated by $\sim 9 \pm 0.5$ ps (a slight non-periodicity in the time separation between the consecutive pump pulses results from slight angular deviations of consecutive pulses from the etalon). This modulation speed is already an order of magnitude higher than the fastest semiconductor lasers reported to date. The figure also shows the laser response to a 15-ps-repetition pump, where the streak-camera resolution more clearly separates the pulses. For practical applications, electrical pumping will be important. Recently, electrical pumping of the nanocavity lasers has been demonstrated[15]. For high-speed electrical modulation, the RC time constants of the lasers have to be small enough, where C and R are the capacitance and resistance of the laser. We believe that very fast electrical pumping of nanocavity lasers is possible, as a recent experiment achieved time constants below 10 ps using micron-scale contacts with sub-fF capacitance[27]. In addition, photonic crystal

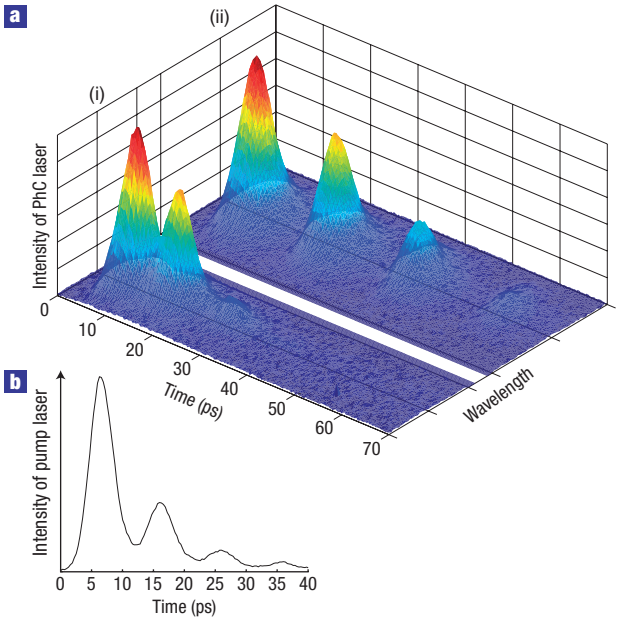

Figure 5 Direct modulation of a single-defect photonic crystal nanocavity laser. **a**, The direct modulation was carried out with the repetition periods of 9 ± 0.5 ps (i) and 15 ps (ii). **b**, A series of femtosecond pump pulses separated by 9 ± 0.5 ps (used to pump i in **a**), obtained by an etalon. The transmitted power of consecutive pulses from the etalon drops geometrically with the ratio $R_1 R_2$ of the mirror reflectivities. Only the first three pump pulses had sufficient power to turn on the laser. Both the femtosecond pump pulses and the laser output pulses are broader as a result of the slow response time of the streak camera.

nanocavity lasers do not require highly resistive Bragg mirror layers, which also limit electrical modulation speeds in fast vertical cavity surface-emitting lasers.

These novel types of nanocavity lasers, built to exploit cavity-QED effects for high speed and lower pump power, could lead to a new generation of lasers with applications in communications and computing. The easy integrability of nanocavity lasers with other photonic components, such as with photonic crystal waveguides, also promises to advance photonic integrated circuits significantly.

Received 24 April 2006; accepted 1 June 2006; published 1 July 2006.

References

1. Purcell, E. Spontaneous emission probabilities at radio frequencies. *Phys. Rev.* **69,** 681 (1946).
2. Yablonovitch, E. Inhibited spontaneous emission in solid-state physics and electronics. *Phys. Rev. Lett.* **58,** 2059–2062 (1987).
3. John, S. Strong localization of photons in certain disordered dielectric superlattices. *Phys. Rev. Lett.* **58,** 2486–2489 (1987).
4. Englund, D. *et al.* Controlling the spontaneous emission rate of single quantum dots in a 2D photonic crystal. *Phys. Rev. Lett.* **95,** 013904 (2005).
5. Badolato, A. *et al.* Deterministic coupling of single quantum dots to single nanocavity modes. *Science* **308,** 1158–1161 (2005).
6. Yoshie, T. *et al.* Vacuum Rabi splitting with a single quantum dot in a photonic crystal nanocavity. *Nature* **432,** 200–203 (2004).
7. Khitrova, G., Gibbs, H. M., Kira, M., Koch, S. W. & Scherer, A. Vacuum Rabi splitting in semiconductors. *Nature Phys.* **2,** 81–90 (2006).
8. Goldstein, E. & Meystre, P. in *Spontaneous Emission and Laser Oscillations in Microcavities* (eds Yokoyama, H. & Ujihara, K.) 1–46 (CRC, New York, 1995).
9. Lodahl, P. *et al.* Controlling the dynamics of spontaneous emission from quantum dots by photonic crystals. *Nature* **430,** 654–657 (2004).
10. Happ, T. D. *et al.* Enhanced light emission of In × Ga12 × As quantum dots in a two-dimensional photonic-crystal defect microcavity. *Phys. Rev. B* **66,** 041303 (2002).
11. Gibbs, H. M. in *Optics of Semiconductors and Their Nanostructures* (eds Kalt, H. & Hetterich, M.) 189–208 (Springer, Berlin, 2004).
12. Cheng, W. H. *et al.* Efficient single-photon sources based on low-density quantum dots in photonic-crystal nanocavities. *Phys. Rev. Lett.* **96,** 117401 (2006).
13. Painter, O. *et al.* Two-dimensional photonic band-gap defect mode laser. *Science* **284,** 1819–1821 (1999).
14. Loncar, M., Yoshie, T., Scherer, A., Gogna, P. & Qiu, Y. Low-threshold photonic crystal laser. *Appl. Phys. Lett.* **81,** 2680–2682 (2002).
15. Park, H. G. *et al.* Electrically driven single-cell photonic crystal laser. *Science* **305,** 1444–1447 (2004).
16. Baba, T. *et al.* Observation of fast spontaneous emission decay in GaInAsP photonic crystal point defect nanocavity at room temperature. *Appl. Phys. Lett.* **85,** 3889–3891 (2004).
17. Yoshie, T., Loncar, M. & Scherer, A. High frequency oscillation in photonic crystal naolasers. *Appl. Phys. Lett.* **84,** 3543–3545 (2004).
18. Deng, H. *et al.* Transverse and temporal mode dependence on mirror contrast in microcavity lasers. *J. Quantum Electron.* **31,** 2026–2036 (1995).
19. Deng, H., Deng, Q. & Deppe, D. G. Very small oxide-confined vertical-cavity surface-emitting lasers with a bulk active region. *Appl. Phys. Lett.* **70,** 741–743 (1997).
20. Coldren, L. A. & Corzine, S. W. *Diode Lasers and Photonic Integrated Circuits* (Wiley, New York, 1995).
21. Chang, C., Chrostowski, L. & Chang-Hasnain, C. J. Injection-locking of vertical cavity surface emitting lasers: Theory and experiments. *J. Sel. Top. Quantum Electron.* **9,** 1386–1392 (2003).
22. Lear, K. L. *et al.* Small and large signal modulation of 850 nm oxide-confined vertical-cavity surface-emitting lasers. *Advances in Vertical Cavity Surface Emitting Lasers in Trends in Optics and Photonics Series* **15,** 69–74 (1997).
23. Yamamoto, Y., Machida, S. & Bjork, G. Microcavity semiconductor laser with enchanced spontaneous emission. *Phys. Rev. A* **44,** 657–668 (1991).
24. Song, B., Noda, S., Asano, T. & Akahane, Y. Ultra-high Q photonic double-heterostructure nanocavity. *Nature Mater.* **4,** 2007–2010 (2005).
25. Altug, H. & Vuckovic, J. Two-dimensional coupled photonic crystal resonator arrays. *Appl. Phys. Lett.* **84,** 161–163 (2004).
26. Altug, H. & Vuckovic, J. Photonic crystal nanocavity array laser. *Opt. Express* **13,** 8820–8828 (2005).
27. Schmidt, R. *et al.* Fabrication of genuine single-quantum-dot light-emitting diodes. *Appl. Phys. Lett.* **88,** 121115 (2006).

Acknowledgements

This work has been supported by the MARCO IFC Center, NSF Grant Nos ECS-0424080 and ECS-0421483, the MURI Center for Photonic Quantum Information Systems (ARO/DTO Program No. DAAD19-03-1-0199), as well as Intel (H.A.) and NDSEG (D.E.) Fellowships.
Correspondence and requests for materials should be addressed to H.A.

Competing financial interests

The authors declare that they have no competing financial interests.